Title: Non-linear stress-softening of the bacterial cell wall confers cell shape homeostasis

Authors: Paola Bardetti[1], Felix Barber[1], Enrique R. Rojas[1,*]

Affiliations:

[1] Department of Biology, New York University, New York, New York, 10003, USA

*Corresponding author. Email: rojas@nyu.edu

Abstract: The bacillus - or rod - is a pervasive cellular morphology among bacteria. Rod-shaped bacteria elongate without widening by reinforcing their cell wall anisotropically, along the cell's circumference, but it is unknown how cells adaptively tune anisotropy to homeostatically control cell width. Through super-resolution measurements of cell wall mechanical properties, we discovered that the *Bacillus subtilis* cell wall exhibits non-linear stress-softening exclusively in the circumferential direction. Furthermore, during steady-state growth the cell wall is inflated precisely to the acute non-linear transition. Physics-based theory correctly predicted that this transition underlies the negative feedback that governs cell width homeostasis. In other words, the cell wall is a "smart material" whose exotic mechanical properties are exquisitely adapted to execute cellular morphogenesis.

28 **Main Text:**

29 **Introduction**

30 The peptidoglycan cell wall is a covalently cross-linked polymer network that defines the size and
31 shape of bacterial cells (Fig. 1A). Three processes mediate expansion of the wall during cell
32 growth: peptidoglycan synthesis[1], enzymatic hydrolysis of the peptide moieties[2], and mechanical
33 deformation of the wall by the large intracellular turgor pressure[3] (≈1-30 atm, depending on
34 species[4, 5]). The primary protein machinery that executes peptidoglycan synthesis during the
35 growth of rod-shaped bacteria is the Rod complex, a heterocomplex of 5 proteins that is scaffolded
36 by oligomers of bacterial actin-homologues[6-8]. These transmembrane complexes synthesize
37 peptidoglycan processively, resulting in anisotropic cell wall microstructure in which the glycan
38 moieties are oriented approximately circumferentially[9] (θ, Fig. 1A) and are connected to one
39 another via the peptide moieties.

40 It is widely believed that the oriented glycans polymers promote rod-shaped growth by
41 mechanically reinforcing the cell wall in the circumferential direction, effectively "girdling" the
42 cell to prevent turgor pressure from driving cell widening[10]. It is also commonly assumed that
43 peptides are oriented longitudinally[11] (l, Fig. 1A). If so, hydrolysis of load-bearing peptides would
44 tend to cause cellular elongation rather than widening.

45 However, this model is not sufficient to explain rod-shaped morphogenesis. Glycans are not
46 oriented strictly circumferentially[9] nor are they infinitely stiff[4]. Similarly, peptides are not oriented
47 strictly longitudinally, and in Gram-positive bacteria the requirement for peptides to connect
48 glycans across the thickness of the cell wall make this impossible. Finally, inflation of the cell by
49 turgor pressure causes anisotropic surface tension in the cell wall whereby the circumferential

50 tension is twice the longitudinal tension[12] ($\lambda_\theta = 2\lambda_l$; Fig. 1A). Therefore, based on first principles,
51 hydrolysis of peptide moieties during cell growth is expected to lead to both elongation and
52 widening.

53 **Peptide hydrolysis causes cell widening**

54 To explicitly demonstrate this principle, we measured the change in cell width in response to
55 exogenous digestion of cell-wall peptides in the Gram-positive bacterium *Bacillus subtilis*. To do
56 so, we used microfluidics to acutely perfuse single bacterial cells with a purified recombinant
57 amidase (Fig. 1A) derived from the lytic bacteriophage SPP1[13]. We labeled the cell wall with a
58 fluorescent D-amino acid[14] and developed a super-resolution method to quantify nanometer-scale
59 changes in cell width (Fig. 1B,C). As hypothesized, amidase perfusion led to a dose-dependent
60 increase in width (Fig. 1D). Surprisingly, when controlling for cell growth, amidase also caused
61 a decrease in cell length (Fig. 1E, *Methods*). Perfusion of lysozyme, which digests the glycan
62 moieties led to the same qualitative effects (Fig. S1A,B).

63 As an alternative method to measure the effect of hydrolysis on cell width, we perfused cells with
64 an inhibitory concentration of vancomycin, which prevents cell wall synthesis without completely
65 inhibiting hydrolysis[15], leading eventually to lysis (Fig. S1C). This treatment also caused cell
66 widening even before it had an effect on elongation rate (Fig. 1F,S1C). Together, these data
67 indicate that peptidoglycan hydrolysis, when unbalanced by synthesis, leads to cell widening.

68 In light of these data, we hypothesized that to avoid slow increases in cell width during the
69 peptidoglycan hydrolysis required for cell growth, cells exert a radially constrictive force on the
70 cell wall that opposes turgor pressure. It was previously shown computationally that applying pre-
71 tension to nascent glycan polymers could prevent pressure-driven widening[16], but this mechanism

was not tested, nor is there an obvious molecular motor within the Rod complex that could exert tension on the cell wall.

Bacteria exhibit finger-trap mechanics

To probe the magnitude of the constrictive force that would be required to counteract inflation, we first measured the mechanical properties of the cell wall. Atomic force microscopy is commonly used to measure the deformation of the cell wall in response to indentation forces[4], but the wall's deformation with respect to changes in surface tension is more relevant to cellular morphogenesis. We therefore subjected *B. subtilis* cells to a microfluidics-based "osmotic force-extension" assay that we previously developed for Gram-negative bacteria[17]. In this assay, single cells are subjected to a series of osmotic shocks (Fig. 2A), which cause acute changes in pressure. These pressure variations deform the cell wall (Fig. 2B), and the dependence of this deformation (the longitudinal and circumferential strains, ε_l and ε_θ) on shock magnitude yields an empirical measurement of the anisotropic mechanical properties of the cell wall (Fig. 2C,D,E).

As expected, hyperosmotic shocks, which decrease pressure, caused longitudinal contraction of the cell wall (negative longitudinal strain, $\varepsilon_l < 0$), whereas hypoosmotic shocks caused longitudinal stretching ($\varepsilon_l > 0$). Moreover, longitudinal strain was inversely proportional to shock magnitude and reversible (Fig. 2B,C), demonstrating that the cell wall is linearly elastic in this dimension.

As expected, small hypoosmotic shocks, which increase turgor pressure, caused circumferential stretching of the cell wall (Fig. 2C). Counterintuitively, small hyperosmotic shocks also caused circumferential stretching. As a result, in this regime variation in pressure had the opposite effect on cell length and width, similar to the effect of peptidoglycan hydrolysis (Fig. 1D,E,S1A,B). This

behavior is reminiscent of a finger-trap toy in which longitudinal tension causes circumferential constriction due to mechanical coupling between the two directions (Fig. 2D). Finger-trap mechanics are more surprising in the case of a pressurized cell where the circumferential surface tension is twice that of the longitudinal tension (Fig. 1A).

Bacterial cells exhibited linear finger-trap behavior for hyperosmotic shocks up to 400 mM (Fig 2C), however, we observed dramatic non-linear behavior outside this range. First, for hyperosmotic shocks between $400 - 800$ mM, the circumferential strain plateaued. At ≈800 mM, we observed a sharp decrease in strain, whereas for larger shocks circumferential strain decreased linearly. Second, since small hypoosmotic shocks caused swelling of cell width, steady-state growth occurs precisely at a sharp non-linear transition.

The cell wall exhibits anisotropic stress-stiffening and -softening

Because the dependence of mechanical strains were approximately linear within the low-pressure and finger-trap mechanical regimes, it was instructive to use linear elasticity theory to interpret these data. For an anisotropic two-dimensional material, linear elasticity can be expressed:

$$\begin{pmatrix} \varepsilon_l \\ \varepsilon_\theta \end{pmatrix} = \frac{1}{E_l} \frac{1}{\alpha(\alpha^{-1} - \nu^2)} \begin{pmatrix} 1 & -\nu \\ -\nu & \alpha^{-1} \end{pmatrix} \begin{pmatrix} \lambda_l \\ \lambda_\theta \end{pmatrix}$$

where E_l is the longitudinal elastic modulus (in 2D), $\alpha = E_\theta / E_l$ is the mechanical anisotropy (ratio of the principal elastic moduli), and ν is similar to the Poisson ratio (*Methods*). The surface tensions, $\lambda_l = PR/2$ and $\lambda_\theta = PR$, balance pressure[12]. Imposing the condition that ε_l and ε_θ have opposite signs when pressure is altered reveals that the cell behaves as a finger trap if $\alpha^{-1} < \nu/2$, that is, if the cell wall is sufficiently anisotropic (Fig. 2F).

Although the empirical dependence of the strains on osmotic shock magnitude (Fig. 2C,D) does not uniquely define α and ν, it constrains them to a slice of parameter space (Fig. 2F). In the finger-trap regime, this analysis demonstrates that the effective Poisson ratio is between $0.45 < \nu < 0.5$ and α is as high as is physically possible within that range, assuming there is no other source of tension other than pressure.

A similar analysis for the mechanical behavior in the low-pressure regime demonstrates that the cell wall has a lower value of anisotropy than in the finger trap regime (Fig. 2F). Since the linear dependence of the longitudinal strain is independent of pressure (Fig. 2C), this means that the transition from the low-pressure regime to the finger-trap regime reflects anisotropic stress-stiffening[4] exclusively in the circumferential direction.

The observation that cells do not behave as a finger trap for hypoosmotic shocks indicate that the wall is softening in the circumferential direction when pressure is increased beyond its steady-state value. We estimated the degree of softening for small increases in pressure, which revealed that the cell wall is quantitatively much softer in this regime than it is in the finger trap regime or the low-pressure regime (Fig. 2F). Therefore, the cell wall undergoes anisotropic (circumferential) stress-stiffening and stress-softening at different critical values of pressure (Fig. 2C).

These data suggest a qualitative model of *B. subtilis* cell wall mechanics (Fig. 2G). First, at low pressures the cell wall is relatively soft in the circumferential direction because the glycan moieties are not fully extended (circumferential strain is low). For example, the glycans may be in folded conformations. In this soft state, the glycans can be thought of as circumferential slack. Therefore, increasing pressure causes the cell wall to stretch circumferentially, and causes the cell to widen. However, eventually the glycans undergo conventional stress-stiffening (they become taut), causing the wall to stiffen in the circumferential direction and leading to finger-trap mechanics. In

137 this state, as pressure increases the cell wall contracts circumferentially, decreasing cell width.
138 Finally, this contraction eventually causes glycans to exit their taut state, leading to softening of
139 the cell wall in the circumferential direction and loss of finger-trap mechanics. Further increase
140 of pressure causes cell widening. In this model, not only does finger-trap behavior inherently
141 depend on mechanical coupling between the longitudinal and circumferential coupling, but the
142 circumferential stiffening and softening must also depend on longitudinal strain since otherwise as
143 soon as the finger trap was engaged it would contract the wall out of the finger-trap regime.

144 **Finger-trap mechanics are correlated with cell-width control**

145 Because finger-trap mechanics correspond to constriction of cell width upon elongation, our results
146 raised the possibility that this behavior was required to avoid runaway widening during cell
147 growth. To explore this hypothesis theoretically, we first constructed a simple physical model for
148 the irreversible mechanical expansion of a linear elastic layered cell wall that accounts for variation
149 of cell length and width (Fig. 3A). The specific spatial relationship of peptidoglycan synthesis and
150 hydrolysis during cell growth is unknown, but since rod complexes are membrane-bound it is
151 believed that synthesis of non-load-bearing peptidoglycan occurs proximal to the membrane
152 whereas the hydrolysis of load-bearing peptidoglycan required for cell growth occurs distally[18].
153 We therefore considered a model in which anisotropic peptidoglycan is added to the inner face of
154 the cell wall at a constant rate and removed at the same rate from the outer face via hydrolysis
155 (*Methods*). Since the cell wall is under tension, removal of load-bearing peptidoglycan dissipates
156 energy and causes irreversible deformation, or growth.

157 When we solved this model computationally across α and ν, we found that the region of parameter
158 space in which cell width decreases dynamically was identical to the region where the cell wall
159 behaves as a finger trap mechanically (compare Fig. 3B to 2F). Similarly, in the region of

160 parameter space where cell width increases upon inflation, the cell widens during simulations of
161 cell growth. The reason for the correspondence between the elastic behavior and growth-dynamics
162 is simple: when load-bearing peptidoglycan is removed from the cell wall, the wall must deform
163 in order to balance pressure, and since we analyzed a linear model, the cell wall deforms as a finger
164 trap regardless of the strain distribution along the proximo-distal axis (Fig. 3A).

165 Therefore, our model made the strong prediction that the cell wall must behave as a finger trap,
166 mechanically, in order to maintain rod shape during growth. We tested this explicitly by
167 genetically manipulating cell-wall mechanical properties and measuring the effect on cell width.
168 It is not possible to tune the Poisson ratio (ν) independently, the anisotropy of the cell wall can be
169 systematically altered by titrating components of Rod complex (specifically the *mreBCD* operon)
170 via inducible expression[19]. When biosynthetic flux through the Rod complex is reduced, the
171 balance is accommodated by PBP1, a non-essential enzyme that synthesizes peptidoglycan
172 isotropically (Fig. 1A). Therefore, when the relative expression of the Rod complex is reduced
173 beyond wild-type levels, cell width acutely increases and cells partially lose rod shape (Fig. 3C).

174 As our model predicted, for Rod complex expression high enough to generate well-shaped rods,
175 modest hyperosmotic shock led to circumferential stretching (finger trap mechanics; Fig. 3D).
176 Conversely, when Rod complex expression was reduced below this threshold cells began to lose
177 rod shape and no longer stretched circumferentially upon hyperosmotic shock. That is, there was
178 a precise correlation between whether the cell maintained a rod shape and whether the cell
179 exhibited finger-trap mechanics. Importantly, for an induction level of 0.5 mM, well below that
180 required for rod-shaped growth, linear elasticity analysis reveals that the cell wall is still highly
181 anisotropic (α>4), demonstrating that finger-trap mechanics, rather than anisotropy alone, is the
182 critical factor underlying the mechanics of rod-shaped morphogenesis.

183 **Pressure-induced wall softening confers width homeostasis**

184 Our analysis explained how cells avoid inflationary widening during cell growth, but the dynamics
185 of this model are inherently unstable: if the cell wall is not a finger trap then the cell widens *ad*
186 *infinitum* during growth, whereas if the wall is a finger trap then cell width asymptotically
187 approaches zero during growth (Fig. 3B).

188 However, the linear model ignored the non-linear stress-softening transition (Fig. 2D).
189 Conspicuously, during steady-state growth the cell wall is inflated precisely to this transition.
190 Given this observation, we posited that the transition could confer an intrinsic mechanism for
191 homeostatic control of cell width if there was feedback between cell width, pressure, and/or the
192 mechanical properties of the cell wall (e.g. the critical pressure at which the transition occurs).
193 More specifically, we hypothesized that during steady-state growth cell width is constant because
194 cells are inflated to the non-linear transition, where neither the finger trap nor stress-softening
195 dominate width dynamics. Accordingly, we predicted that for cells that are wider than their steady-
196 steady width but are dynamically thinning (i.e., relaxing to steady-state, Fig. S2), that the cell wall
197 would be in the finger trap regime.

198 To test this, we cultured cells to steady-state growth at low Rod-complex expression, acutely
199 induced high Rod-complex expression, and then performed circumferential osmotic-force-
200 extension experiments before, during, and after relaxation to steady-state. As for wild-type
201 bacteria, both hypo- and hyperosmotic shocks caused swelling of width for cells grown to steady-
202 state at low, medium, and high Rod complex expression (Fig. 4A-C). However, as we
203 hypothesized, hypoosmotic shocks up to 600 mM caused constriction of cell width for cells that
204 were actively thinning (Fig. 4C). In other words, during cell thinning the cell wall was squarely

205 in the finger trap regime. The validation of this non-intuitive prediction strongly supports our
206 model that the non-linear properties of the cell wall govern width dynamics.

207 Our observation that the cell wall is in the finger trap regime during thinning but not during steady-
208 state growth suggested that turgor pressure is variable during width dynamics. In this light, we
209 next interrogated the nature of the feedback that underlies the adaptation of cell wall mechanical
210 properties during width homeostasis. Since finger trap-mediated cell thinning occurs when turgor
211 pressure is lower than the critical stress-softening pressure, we considered two hypotheses for the
212 mechanism of cell width homeostasis: i) that thinning leads to increased pressure, or ii) thinning
213 leads to a decrease of in the critical stress-softening pressure. Either of these processes would
214 complete a negative feedback loop.

215 To measure pressure, we performed our longitudinal osmotic-force-extension assay (Fig. 2C), and
216 in a second experiment we lysed cells and measured length contraction upon loss of turgor
217 pressure; we thus quantified the magnitude of hyperosmotic shock that caused contraction of the
218 cell wall to the same length as cell lysis, which gives an empirical measurement of turgor pressure
219 in units of osmolarity (Fig. 4D).

220 Contrary to our initial expectations, we found that turgor pressure was inversely dependent on Rod
221 complex expression (Fig. 4E). This corresponded to a positive correlation between pressure and
222 cell width during steady-state growth. Since, at steady-state, cells are inflated to the non-linear
223 stress-softening transition regardless of Rod complex expression level, these measurements led us
224 to a surprising conclusion: that the critical stress-softening pressure is dynamically variable.

225 Despite the correlation between pressure and cell width during steady-state growth, upon acute
226 induction of Rod complex expression pressure equilibrated to its low, steady-state value faster than

227 cell width or the critical pressure of the non-linear transition (Fig. 4C,E), implying that pressure is
228 directly dependent on the specific molecular architecture of the cell wall rather than directly on
229 width. In concurrent work, we identified a molecular mechanism by which *B. subtilis* directly
230 senses cell wall microstructure and relays this information to the osmoregulation systems via
231 cyclic-di-AMP signaling, which could underlie these observations.

232 Together, our data are consistent with a hybrid feedback system that incorporates molecular and
233 mechanical signals to ensure cell width homeostasis (Fig. 4F,G). According to this model, both
234 turgor pressure and the critical pressure at which the non-linear stress-softening transition are key
235 dynamical variables. If cells are wider than their target steady-state value, then the critical pressure
236 is higher than the actual pressure, the cell wall is in the finger trap regime, and cells thin
237 dynamically. According to our model, thinning causes the critical pressure to decrease until it
238 reaches the actual pressure; further thinning would cause the critical pressure to decrease beyond
239 the actual pressure, positioning the cell wall in the stress-softened regime, which would cause them
240 to widen, completing the negative feedback.

241 **Finger-trap mechanics are unique to Gram-positive rod-shaped bacteria**

242 We tested the generality of the finger-trap mechanism of cell width control across other bacteria.
243 Interestingly, *Corynebacterium glutamicum*, another rod-shaped Gram-positive bacterium does
244 not exhibit finger trap mechanics for hyperosmotic shocks. This makes sense, however, since *C.*
245 *glutamicum* elongates via polar growth rather than the diffuse growth used by *B. subtilis*: for polar
246 growth, cell width must be maintained through control of the size of the polar growth zone.
247 Previous measurements of *E. coli* cell geometry in response to osmotic shocks did not indicate
248 finger-trap mechanics[20], a result we confirmed (Fig. 4H). This suggests that Gram-negative

249 bacteria must also use another mechanism to control width in spite of turgor pressure, which is
250 however much lower than in Gram-positive bacteria[4].

251

252 **Discussion**

253 Transduction of forces within eukaryotic cells is mediated by molecular mechanosensors[21] that
254 elicit biochemical and genetic responses that can, in turn, manipulate forces within the cell. For
255 example, when force is applied to branched actin networks, the network rapidly increases the
256 amount of force it can sustain through structural alterations to the network, a process that is hard-
257 wired into the biochemistry of actin-binding proteins[22]. Like actin, we found that the Gram-
258 positive bacterial cell wall is a "smart material" that internally senses and responds to forces.
259 However, the cell wall employs a quintessentially prokaryotic paradigm whereby negative-
260 feedback regulation of cell width is embedded the exotic non-linear properties of the wall.

261 A major open question motivated by our discovery is the specific mechanism by which the critical
262 pressure at which the non-linear transition occurs depends on cell width. We hypothesize that a
263 key variable that is missing from our model is the surface area-to-mass ratio, which determines the
264 metabolic flux through the peptidoglycan biosynthesis pathway[15]. For example, the critical
265 pressure could depend on the quantitative ratio between this flux and that of peptidoglycan
266 hydrolysis, which is less likely to depend on cell width. Building upon our analysis, such a
267 mechanism would provide scaling relationships that predict how cell width quantitatively depends
268 on environmental variables including nutrients and osmotic pressure.

269

Acknowledgements

We thank Ethan Garner and Carlos São-José for strains, plasmids, technical assistance, and helpful discussions.

Funding

National Institutes of Health R35GM143057 (ER, PB).

Competing interests

The authors declare no competing interests.

Supplementary Materials

Materials and Methods

Figs. S1 and S2

Table S1

References and Notes

1. Typas (2012) From the regulation of peptidoglycan synthesis to bacterial growth and morphology. *Nature Reviews Microbiology.* 10(2).

2. Vollmer (2008) Bacterial peptidoglycan (murein) hydrolases. *FEMS Microbiol Rev.* 32(2).

3. Rojas (2017) Homeostatic Cell Growth Is Accomplished Mechanically through Membrane Tension Inhibition of Cell-Wall Synthesis. *Cell Syst.* 5(6).

4. Deng (2011) Direct measurement of cell wall stress stiffening and turgor pressure in live bacterial cells. *Phys Rev Lett.* 107(15).

5. Whatmore (1990) Determination of turgor pressure in Bacillus subtilis: a possible role for K+ in turgor regulation. *Microbiology.* 136(12).

6. Garner (2021) Toward a mechanistic understanding of bacterial rod shape formation and regulation. *Annual Review of Cell and Developmental Biology.* 37(1).

7. Garner (2011) Coupled, circumferential motions of the cell wall synthesis machinery and MreB filaments in B. subtilis. *Science.* 333(6039).

8. Domínguez-Escobar (2011) Processive movement of MreB-associated cell wall biosynthetic complexes in bacteria. *Science.* 333(6039).

9. Pasquina-Lemonche (2020) The architecture of the Gram-positive bacterial cell wall. *Nature.* 582(7811).

10. Auer (2017) Bacterial cell mechanics. *Biochemistry.* 56(29).

11. Vollmer (2008) Murein (peptidoglycan) structure, architecture and biosynthesis in Escherichia coli. *Biochimica et Biophysica Acta (BBA)-Biomembranes.* 1778(9).

12. Love (1897) *Theoretical mechanics: an introductory treatise on the principles of dynamics with applications and numerous examples*

13. Fernandes (2016) More than a hole: the holin lethal function may be required to fully sensitize bacteria to the lytic action of canonical endolysins. *Molecular microbiology.* 102(1).

14. Kuru (2012) In situ probing of newly synthesized peptidoglycan in live bacteria with fluorescent D-amino acids. *Angewandte Chemie.* 124(50).

15. Kitahara (2022) The role of cell-envelope synthesis for envelope growth and cytoplasmic density in Bacillus subtilis. *PNAS nexus.* 1(4).

16. Furchtgott (2011) Mechanisms for Maintaining Cell-Shape in Rod-Shaped Gram-Negative Bacteria. *Biophysical Journal.* 100(3).

17. Fitzmaurice (2024) β-barrel proteins dictate the effect of core oligosaccharide composition on outer membrane mechanics. *Biophysical Journal.*

18. Koch (1985) Inside-to-outside growth and turnover of the wall of gram-positive rods. *Journal of theoretical biology.* 117(1).

19. Dion (2019) Bacillus subtilis cell diameter is determined by the opposing actions of two distinct cell wall synthetic systems. *Nature Microbiol.* 4(8).

20. Rojas (2014) Response of Escherichia coli growth rate to osmotic shock. *PNAS.* 111(21).

21. Gomez (2021) Molecular paradigms for biological mechanosensing. *The Journal of Physical Chemistry B.* 125(44).

22. Bieling (2016) Force feedback controls motor activity and mechanical properties of self-assembling branched actin networks. *Cell.* 164(1).

Figures

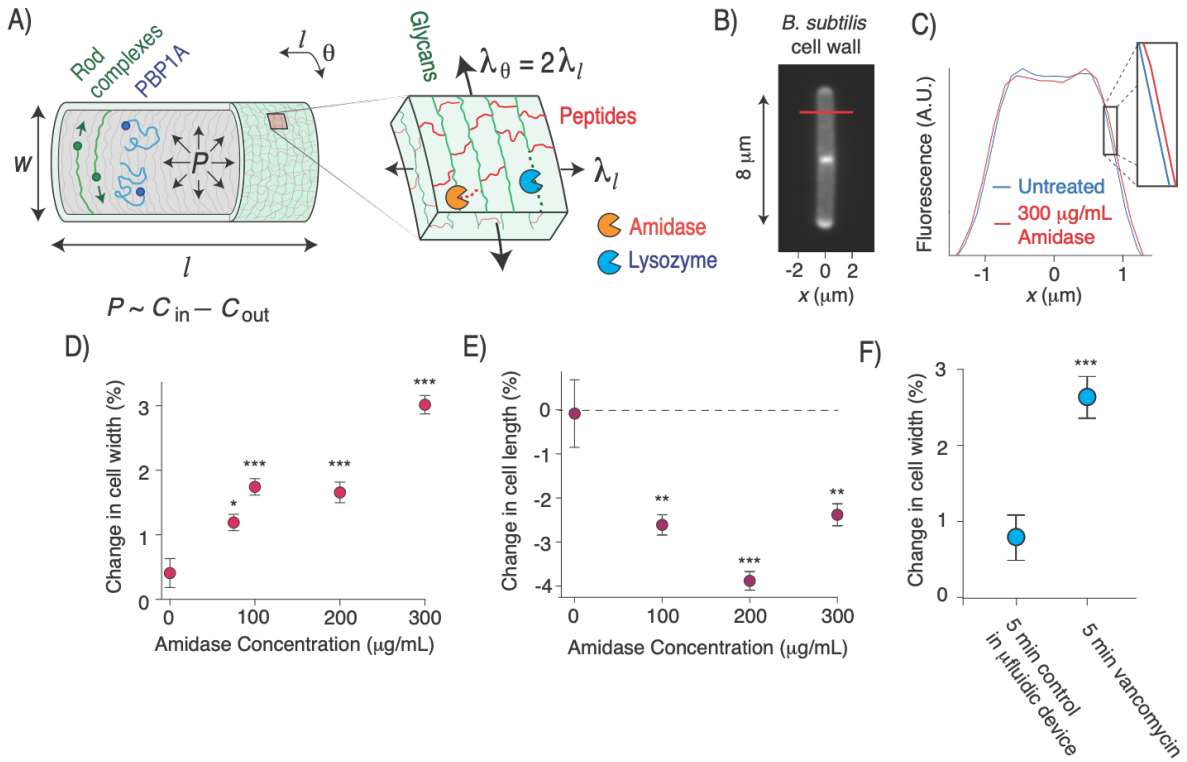

Figure 1. Exogenous peptide digestion causes cell widening. A) Diagram of the Gram-positive cell wall including its modes of synthesis and cell surface co-ordinate system (l,θ). P: turgor pressure. $\lambda_{l,\theta}$ are the longitudinal and circumferential surface tensions. B) *B. subtilis* cell wall labeled with the fluorescent D-amino acid HADA. C) Mean fluorescent profile across the width of the labeled cell wall (red line in B) before and after 30 s amidase treatment. D) Mean change in cell width upon amidase treatment. Error bars indicate +/- 1 s.e.m. n=15-50 cells across two technical replicates per data point. E) Mean change in cell length upon amidase treatment, controlling for cell growth. Error bars indicate +/- 1 s.e.m. n=20-50 cells across two technical replicates per data point. F) Change in cell width during 5 minute of growth in the microfluidic chip (control) and during 5 minutes of treatment with 10 mg/mL vancomycin. *: p=10^{-2},**: 10^{-3},***: p<10^{-4}, compared to untreated control.

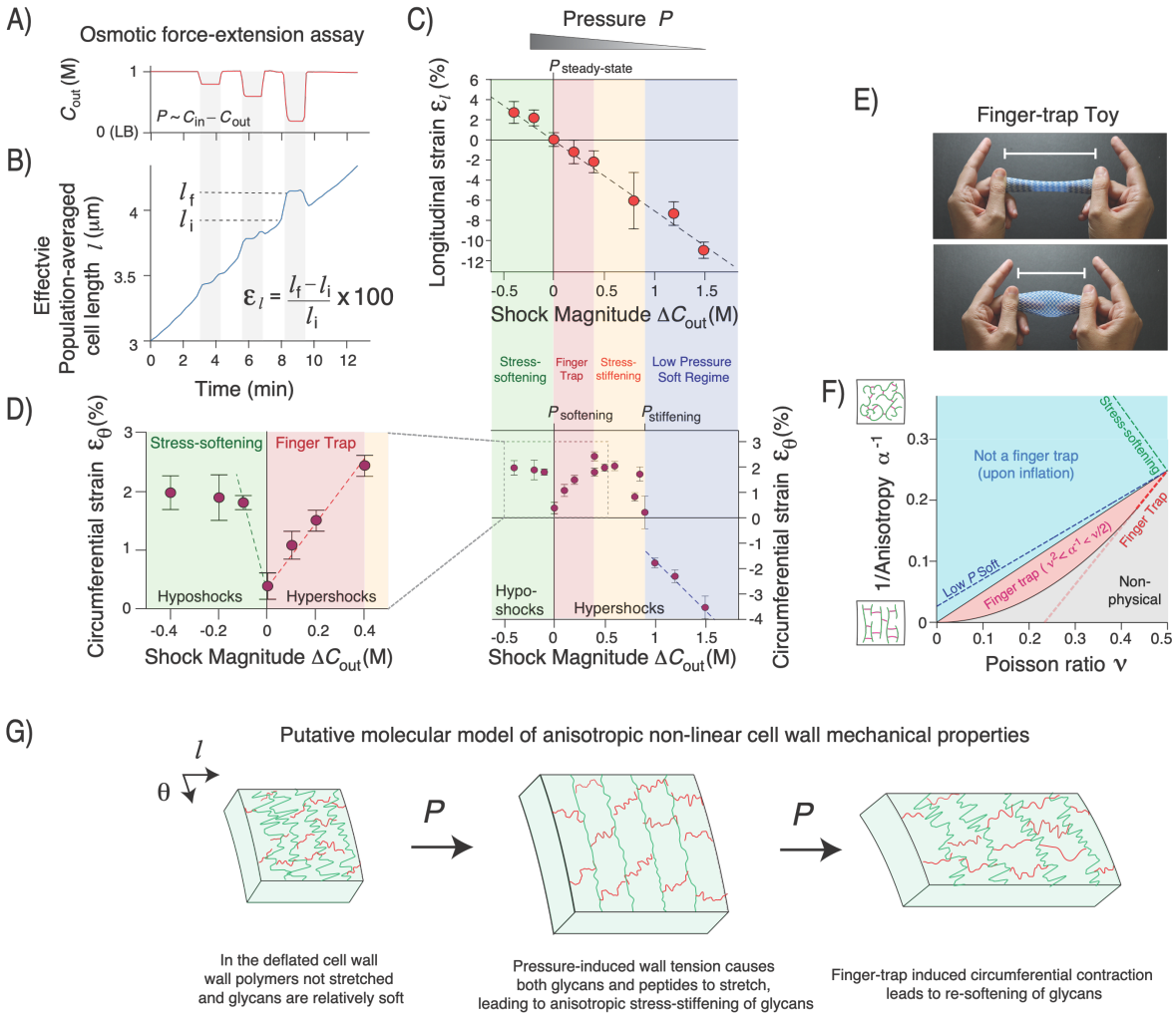

Figure 2. The cell wall exhibits anisotropic stress-stiffening and stress-softening. A) Extracellular concentration of sorbitol, C_{out}, versus time during an osmotic force-extension experiment. B) Effective population-averaged cell length versus time during the osmotic force-extension experiment. C) Longitudinal strain versus shock magnitude across several osmotic force extension experiments. n=20-60 cells across 1-3 replicate experiments per shock magnitude. Error bars: +/- 1 s.e.m. The dotted line is a linear regression. D) Circumferential strain versus shock magnitude across several osmotic force extension experiments. n=74-174 across 1-2 replicate experiments per shock magnitude. Error bars: +/- 1 s.e.m. The dotted lines are linear regressions to the three linear regimes of mechanical behavior. E) A finger trap toy. F) The mechanical behavior of an inflated linear elastic cylindrical cell wall versus its anisotropy and Poisson ratio. The dotted lines are the behavior constrained by slopes of the regressions in C) and D). G) Putative qualitative molecular model of the anisotropic non-linear cell wall mechanical properties.

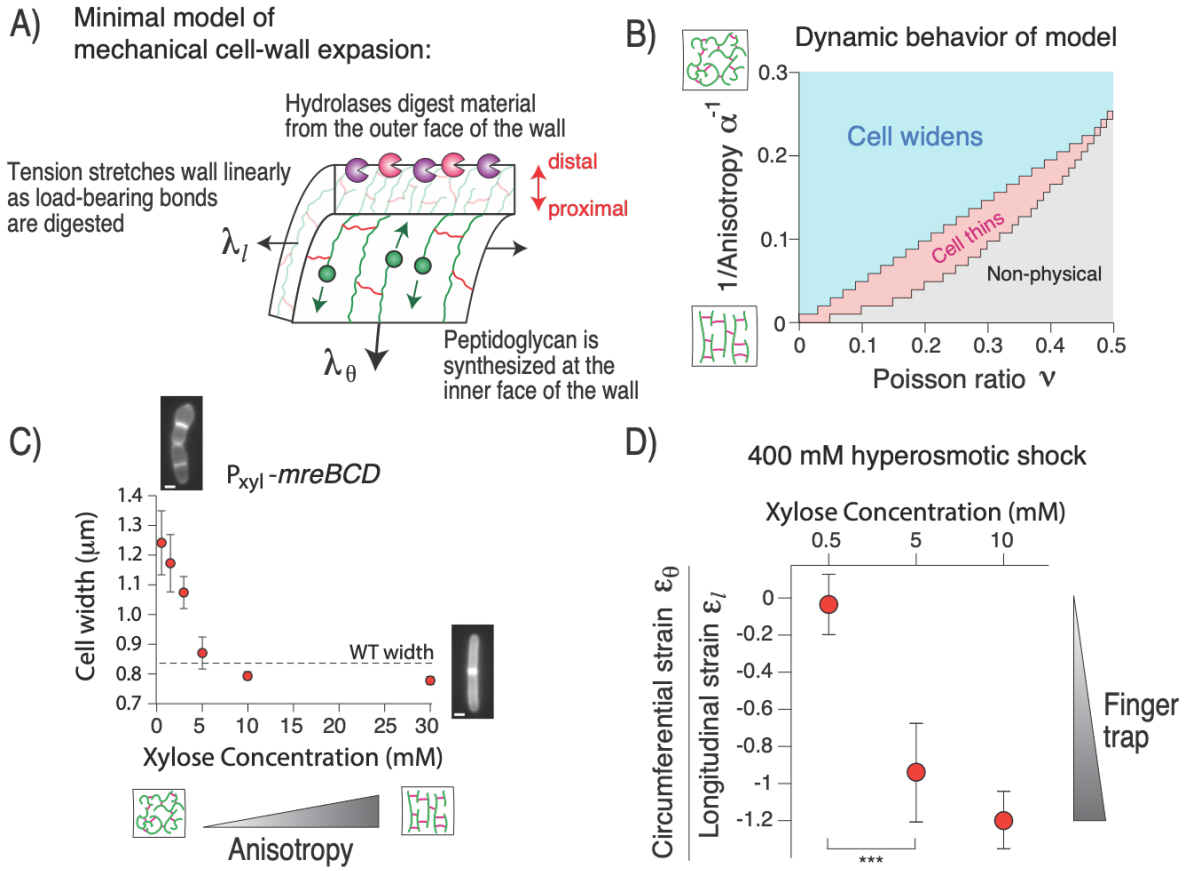

Figure 3. Finger trap mechanics are correlated with cell-width control. A) Diagram of the components of the theoretical linear elastic model for cell growth. B) Dynamic behavior of the model versus the anisotropy and Poisson ratio. C) Cell width versus induction of *mreBCD*. n=22-57 cells across 1 replicate per induction level. Error bars: +/- 1 s.d. D) Ratio of circumferential strain and longitudinal strain upon 400 mM hyperosmotic shock for three induction levels of *mreBCD*. Values were calculated from n=26-90 cells across 1-3 replicate experiments (circumferential strain) and n=60-78 cells across 1 replicate experiment (longitudinal strain) per induction level. Error was propagated from the s.e.m. for each respective measurement. ***: $p<10^{-4}$.

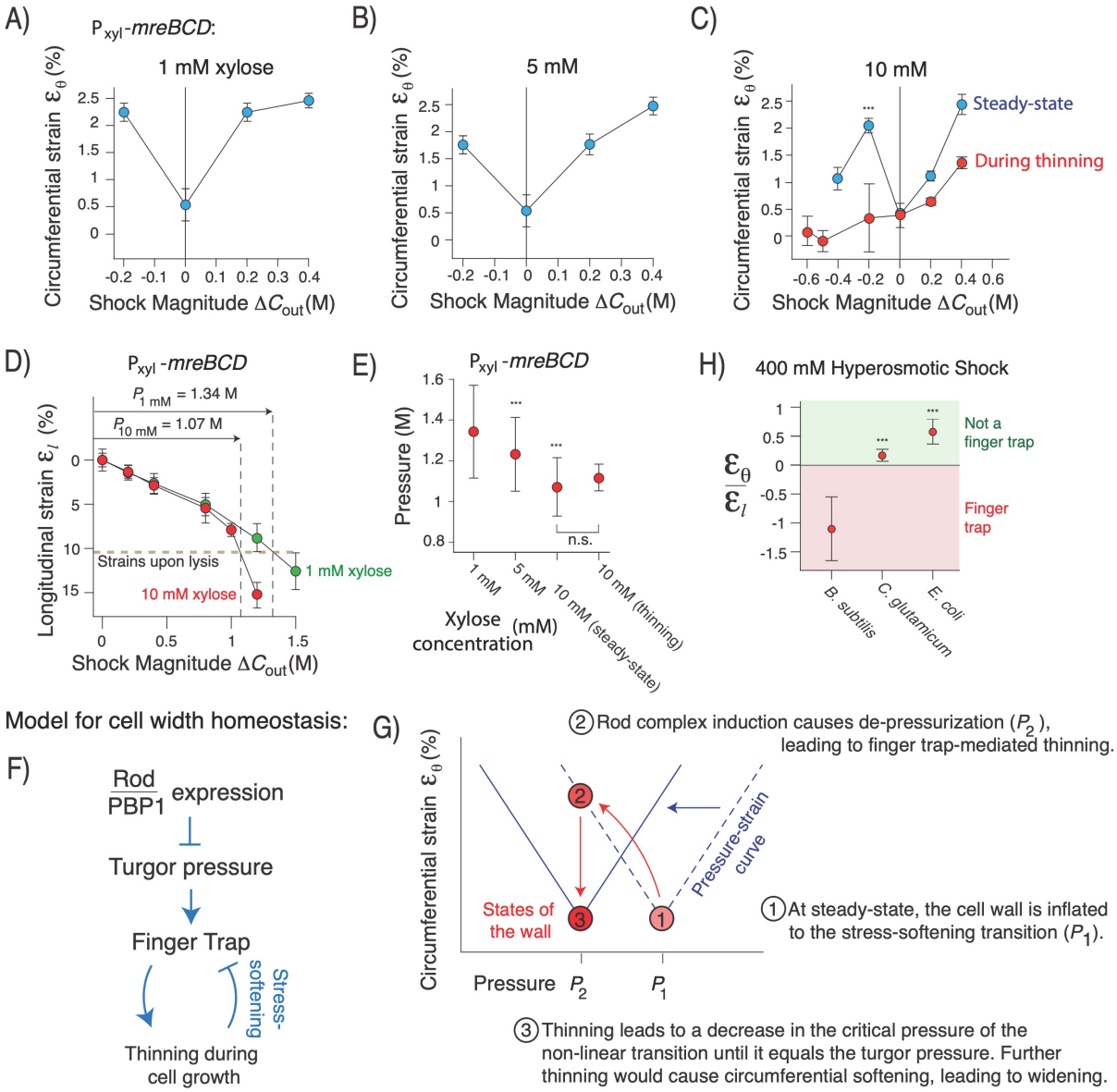

Figure 4. Strain-softening confers cell width homeostasis. Circumferential strain versus shock magnitude at A) 1 mM, B) 5 mM and C) 10 mM xylose induction of P_{xyl}-*mreBCB*. n=30-50 cells across 1-3 replicate experiments per shock magnitude. Error bars: +/- 1 s.e.m. D) Assay to measure turgor pressure by measuring the magnitude of hyperosmotic shock that causes the cell wall to contract to its rest length. n=60-175 cells across 1-2 replicate experiments per shock magnitude. n=73-90 cells across 2 replicate experiments for each lysis strain measurements. E) Mean turgor pressure versus induction of P_{xyl}-*mreBCB* across replicate experiments per induction level. Error was propagated from that of the lysis strain and regression of the osmotic force-extension (*Methods*) F,G) Qualitative negative feedback model of cell width homeostasis based on finger-trap mechanics and stress-softening. H) Ratio of circumferential strain and longitudinal strain upon 400 mM hyperosmotic shock for wild-type *B. subtilis*, *C. glutamicum*, and *E. coli*. *B. subtilis* statistics are the same as in Fig. 2C,D. For *C.g.*: n=20-30 cells across 1 experiment for circumferential strain and n= 306 across 1 experimental for longitudinal strain.

416 For *E.c.*: n=22-37 cells across two experimental replicates for circumferential strain n=238 cells
417 across 3 experimental replicates for longitudinal strain. ***: $p<10^{-4}$, compared to *B. subtilis*.